Spin excitations in frustrated *A*-site spinels investigated with inelastic neutron scattering

A. Krimmel,[1,*] H. Mutka,[2] M. M. Koza,[2] V. Tsurkan,[1,3] and A. Loidl[1]
[1]*Experimental Physics V, Center for Electronic Correlations and Magnetism, Augsburg University, D-86159 Augsburg, Germany*
[2]*Institut Laue Langevin, BP 156 X, F-38042 Grenoble Cedex 9, France*
[3]*Institute of Applied Physics, Academy of Sciences of Moldova, MD2028 Chisinau, R. Moldova*
(Received 7 February 2008; revised manuscript received 12 November 2008; published 3 April 2009)

The magnetic ions of the *A*-site spinels $M\mathrm{Al_2O_4}(M=\mathrm{Mn,Fe,Co})$ form a diamond lattice which, by means of competing interactions, are subject to strong frustration effects. In this paper we present the outcome of inelastic neutron-scattering experiments to investigate the corresponding magnetic excitations. $\mathrm{MnAl_2O_4}$ exhibits the strongest magnetic exchange and reveals long-range magnetic order below $T_N=40$ K with a well-defined spin-wave dispersion. In contrast, $\mathrm{CoAl_2O_4}$ and $\mathrm{FeAl_2O_4}$ do not show long-range order but the magnetic scattering corresponds to a liquidlike structure factor. Inelastic neutron scattering in $\mathrm{CoAl_2O_4}$ shows a dispersionlike structure indicating collective magnetic excitations, despite the absence of long-range magnetic order. This type of behavior corresponds to a cooperative paramagnet. The opening of a spin gap in $\mathrm{FeAl_2O4}$ is observed at low temperatures. These three *A*-site spinels are located on the border of long-range magnetic order with distinct emergent behavior. The corresponding role of orbital degrees of freedom is discussed.

DOI: 10.1103/PhysRevB.79.134406 PACS number(s): 75.40.Gb, 78.70.Nx, 75.30.Et, 67.90.+z

I. INTRODUCTION

Frustrated systems are in focus of current research, due to their highly unusual physical properties. Frustration is characterized by the fact that it is impossible to satisfy all pairwise interactions simultaneously. Spin frustration suppresses long-range magnetic order and strongly enhances spin fluctuations in magnetic materials. The ratio of the Curie-Weiss temperature reflecting the energy scale of the leading magnetic exchange, to the ordering temperature is commonly used as a measure of frustration.[1] The resulting strong degeneracy of the ground state however may be lifted by any additional interaction which enters in a nonperturbative way. This is the origin of a large variety of fascinating complex ground states that becomes available for frustrated systems while depending on the very details of the interactions (e.g., exchange, anisotropy, magnitude of the spin etc.) involved. Spin liquids,[2] spin-ice states,[3,4] clusters or loops of a finite number of spins,[5–7] heavy fermionlike behavior,[8,9] as well as singlet formation[10] are typical examples of these exotic ground states. In some cases as in chromium oxide spinels, magnetic frustration is lifted by means of a coupling between spin and lattice degrees of freedom,[11,12] therefore resulting in a magnetic[13] or spin-driven[14] Jahn-Teller effect.

In regard to spinel compounds of stoichiometry AB_2X_4, the *B* sites form a corner sharing tetrahedral network known as the pyrochlore lattice which exhibits strong geometric frustration, as outlined many years ago by Anderson.[15] The *A*-site sublattice of the spinel structure on the other hand forms a diamond lattice corresponding to two interpenetrating fcc sublattices. Theoretical calculations of the antiferromagnetic (AFM) diamond lattice reveal that frustration arises, due to the competition between the exchange J_2 within an fcc sublattice and the coupling J_1 between them.[16] For a ratio $J_2/J_1<1/8$, an AFM Néel ground state with strongly reduced ordering temperature upon increasing J_2/J_1 is calculated, whereas for $J_1/J_2>1/8$ a spiral spin liquid is formed at low temperatures. Complex magnetic ordering by means of an order by disorder mechanism is established out of this spiral spin liquid,[16] in quantitative agreement with experimental results on $\mathrm{MnSc_2S_4}$.[17] It has been recently shown that frustration of *A*-site spinels affects both the spin and the orbital sector.[18–22] Geometric frustration of orbitals can be inferred experimentally from the observation that a lattice of Jahn-Teller (JT) active magnetic ions does not undergo a cooperative JT transition. In this case the ground state is expected to be an orbital liquid or an orbital glass.[21]

Here we report on neutron-scattering studies of *A*-site spinels $M\mathrm{Al_2O_4}(M=\mathrm{Mn,Fe,Co})$. These compounds crystallize in the normal cubic spinel structure in which the *B* site is occupied by nonmagnetic Al ions. The tetrahedral crystal field at the *A* site splits the 3*d* electron manifold into a lower doublet (*e*) and an excited triplet (t_2) state. Accordingly, the electronic configuration is $S=5/2$, $L=0$ (half-filled shell) for $\mathrm{MnAl_2O_4}$, $S=2$, $L=2$ (hole in the lower doublet, Jahn-Teller active) for $\mathrm{FeAl_2O_4}$ and $S=3/2$, $L=0$ (filled lower doublet) for $\mathrm{CoAl_2O_4}$. Bulk measurements on $M\mathrm{Al_2O_4}(M=\mathrm{Mn,Fe,Co})$ reveal that $\mathrm{MnAl_2O_4}$ orders antiferromagnetically below $T_N=40$ K with a reduced ordered moment and a significant paramagnetic component, whereas $\mathrm{FeAl_2O_4}$ and $\mathrm{CoAl_2O_4}$ reveal spin-glass-like anomalies at $T^*=12$ K(M=Fe) and 4.8 K (M=Co), respectively.[23] These results were confirmed by neutron powder diffraction.[24] A simple colinear AFM structure has been determined for $T<T_N$ in $\mathrm{MnAl_2O_4}$ with an ordered magnetic moment of $3.7\mu_B$ at 1.6 K. This is reduced significantly as compared to $4.9\mu_B$ expected for Mn^{2+}. This reduction is accounted for by diffuse magnetic scattering around the magnetic Bragg reflections and indicate coexisting short-range order down to low temperatures. Both $\mathrm{FeAl_2O_4}$ and $\mathrm{CoAl_2O_4}$ reveal a liquidlike structure factor of the magnetic scattering which corresponds to short-range magnetic order only.[24] These very different ground states occur despite the fact that all three compounds under investigation reveal similar Curie-Weiss temperatures of the order of 100 K. In addition, no experimental evidence has been detected for the onset of orbital order in $\mathrm{FeAl_2O_4}$.

II. EXPERIMENTAL RESULTS AND DISCUSSION

Polycrystalline samples of MAl_2O_4 (M=Fe, Mn, and Co) were prepared by conventional solid-state synthesis of high-purity (99.99%) binary oxides (FeO, MnO, CoO, Co_3O_4, and Al_2O_3) in evacuated quartz ampoules. In order to reduce site intermixing, which strongly increases at high temperatures, the sintering temperature was restricted to 1000 °C. The sintering process was repeated several times to reach full chemical reaction. The sample homogeneity and the absence of foreign phases were checked by x-ray diffraction. All samples were slowly cooled to room temperature with a rate of about 15 °C/h to prevent frozen disorder.

Inelastic neutron-scattering experiments were performed in a temperature range of 1.6 K$<T<$160 K on the time-of-flight spectrometer IN4 at the Institut Laue Langevin, Grenoble, with an incident neutron wavelength of 2.1804 Å. An empty can and a vanadium standard have been additionally measured to account for background and detector efficiency, respectively. The raw data have been corrected in a standard way employing the LAMP program package[25] converting time of flight to energy transfer and a constant Q or constant energy-transfer mapping finally resulting in $S(Q,\omega)$. The large-angle detector bank of the spectrometer covers a range of wave vector transfers of 0.75 Å$^{-1}\leq Q \leq$5.2 Å^{-1} in the elastic channel for the selected wavelength. A small-angle detector was used in addition to extend the measurements to Q values below 0.75 Å^{-1}. However, the small-angle detector and the main detector bank do not merge completely. Therefore, a significant loss of intensity in form of a pronounced bottleneck is observed around this particular wave-vector transfer in the contour plots of $S(Q,\omega)$. The low-Q data have been included in these figures for the sake of completeness, but the data below 0.75 Å^{-1} are not reliable and therefore, do not allow for any additional conclusions. Some additional high-resolution measurements were performed in $FeAl_2O_4$ on the cold time-of-flight spectrometer IN6 using an incident neutron wavelength of 5.1 Å.

The dynamic structure factor $S(Q,\omega,T)$ is directly proportional to the imaginary part of the generalized susceptibility,

$$S(Q,\omega,T)=\hbar\omega(1-e^{-\hbar\omega/k_BT})^{-1}\chi''(Q,\omega,T). \quad (1)$$

The first term represents the detailed balance factor accounting for thermal population. Exponential spin relaxation results in a Lorentzian-shaped quasielastic line of width Γ (multiplied with the detailed balance factor and convoluted with the instrumental resolution),

$$\chi''(Q,\omega,T)=\chi_0(Q,T)\frac{\Gamma(Q,T)}{\omega^2+\Gamma^2(Q,T)}. \quad (2)$$

The dynamic structure factor of all three investigated compounds is well described by a single quasielastic Lorentzian at sufficiently high temperatures ($T\geq$100 K for $MnAl_2O_4$ and $CoAl_2O_4$ and $T\geq$50 K for $FeAl_2O_4$) according to Eqs. (1) and (2). Upon cooling, the quasielastic response of the paramagnetic state becomes inelastic due to increasing magnetic correlations. The low-temperature spectra were fitted by an additional damped harmonic oscillator (DHO) taking into account detail balance and corresponding to a double Lorentzian[26] with oscillator strength A_{DHO}, eigenfrequency ω_{DHO} and linewidth Γ_{DHO},

$$S(Q,\omega)=\frac{A_{\mathrm{DHO}}\omega\Gamma_{\mathrm{DHO}}}{(\omega^2-\omega_{\mathrm{DHO}}^2)^2+(\omega\Gamma_{\mathrm{DHO}})^2}\frac{1}{1-e^{-\hbar\omega/k_BT}}. \quad (3)$$

A single inelastic line is sufficient to describe the data in $FeAl_2O_4$ and $CoAl_2O_4$, whereas in $MnAl_2O_4$, two inelastic lines are necessary to arrive at adequate fits.

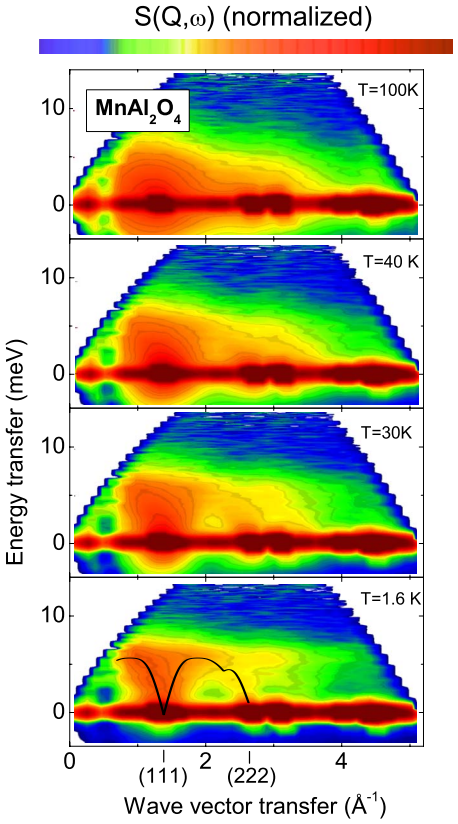

FIG. 1. (Color online) Contour plot of the dynamic structure factor $S(Q,\omega)$ of $MnAl_2O_4$ for various temperatures. Magnetic intensities are shown by a suitable color coding on a logarithmic scale (darker grey upon increasing intensity up to the background level at high energy transfers). The solid line in the lowest frame shows the calculated spin-wave dispersion of $MnAl_2O_4$ along (ξ,ξ,ξ) including nearest- and next-nearest-neighbor ions as described in the text. The Bragg-peak positions of the (111) reflection at 1.33 Å^{-1} and the (222) reflection at 2.65 Å^{-1} are indicated.

A. $MnAl_2O_4$

As outlined above, $MnAl_2O_4$ reveals a simple colinear AFM structure below T_N=40 K with an additional, coexisting paramagnetic component. A contour plot of the dynamic structure factor $S(Q,\omega)$ of $MnAl_2O_4$ is shown in Fig. 1 at various temperatures. The dark red riff around zero energy transfer originates from incoherent scattering with dark spots corresponding to nuclear Bragg reflections. The first five nuclear reflections are (111) at 1.33 Å^{-1}, (220) at 2.17 Å^{-1}, (311) at 2.54 Å^{-1}, (222) at 2.65 Å^{-1}, and (400) at 3.06 Å^{-1}.

Additional magnetic scattering is color coded to indicate increasing intensities from green via yellow and orange to light red above the background level shown in blue. The magnetic intensity extends over an energy-transfer range up to about 10 meV or 116 K (at $Q \approx 1$ Å^{-1}) and reflects the overall energy scale of the magnetic exchange. Within mean-field approximation in the high-temperature Curie-Weiss regime, the Curie-Weiss temperature is given by $\theta_{CW} = zJ_{MF}S(S+1)/3$ with $\theta_{CW} = 143$ K and $z=4$ for tetrahedral coordination of the magnetic *A*-site ions. Taking the experimental value of $\theta_{CW} = 143$ K and considering nearest-neighbor interactions only with $S = 5/2$ results in a mean-field exchange of $J_{MF} = 12.3$ K for $MnAl_2O_4$. It is noted that the calculations of the theoretical phase diagram of the AFM diamond lattice (Fig. 3 of Ref. 16) were performed employing unit vectors for the spin and scaled exchange constants $J_i = J_{MF}S(S+1)$. Accordingly, $J_1 = 107.25$ K and $T_N/J_1 = 0.373$ which results in a ratio of the nearest- and second-nearest-neighbor exchange of approximately $J_2/J_1 \approx 0.09$. This value is smaller but close to the critical ratio of 1/8 at which the AFM Néel state becomes unstable. $MnAl_2O_4$ shows consequently long-range AFM order with a reduced ordering temperature and strongly enhanced spin fluctuations.

We point out that the estimations of the exchange constants are speculative as far as they rely entirely on the theoretical model calculations presented in Ref. 16 which are originally applied to the homolog compound $MnSc_2S_4$. However, we note that the AFM diamond lattice should be generally applicable to *A*-site spinels with spin-only configuration and that no superior alternative scenario has been developed until now.

Having determined the values of the exchange constants allows to calculate the corresponding AFM spin-wave dispersion according to $\hbar\omega(\mathbf{q}) = zJS(1-\gamma_q^2)^{1/2}$ with $\gamma_q = m^{-1}\Sigma_m \exp(i\mathbf{q}\cdot\mathbf{r}_m)$ with the exchange constant $J_1 = 107.25$ K for the four nearest-neighbor ions at a distance $a\sqrt{3}/4$ and $J_2 = 9.65$ K for the 12 next-nearest-neighbor ions at a distance $a/\sqrt{2}$. The prefactor $zJ_{MF}S = 123$ K or 10.6 meV represents the spin-wave bandwidth in reasonable agreement with the experimentally observed energy-transfer range of 10 meV of the magnetic scattering. The resulting normalized magnon dispersion for the three principal cubic directions is shown in Fig. 2. The directional average of powder measurements results strictly in a magnon density of states. A direct comparison with a given model would require the calculation of the entire dispersion surface evenly distributed over the Brillouin zone and its subsequent summation. Therefore we restrict ourselves to a comparison of the measured magnetic excitation spectra with the dispersion relation along the three principal symmetry directions, because a powder average will not significantly change the physical conclusions drawn from this simplified approach. A large excitation gap appears for the $(\xi,\xi,0)$ direction contrary to the experimentally observed spin waves emanating directly from the magnetic Bragg peaks at the zone center. The dispersions along the $(\xi,0,0)$ and (ξ,ξ,ξ) direction look evidently similar without an energy gap. Therefore, we exclude a significant contribution of spin waves along $(\xi,\xi,0)$, in agreement to calculations predicting dominating spiral spin correlations along the (ξ,ξ,ξ) direction for the specific exchange constants of $MnAl_2O_4$. Due to the small ratio of $J_2/J_1 \approx 0.09$, the influence of the next-nearest neighbors is weak and cannot be extracted on the basis of the present powder measurements. The calculated spin-wave dispersion along (ξ,ξ,ξ) is shown in the bottom frame of Fig. 1 including the small contribution of the next-nearest neighbors (corresponding to a small dip in the dispersion curve). It accounts well for the experimentally observed magnetic scattering intensities and the magnon dispersion shown in the lower frame of Fig. 1 extends from the (111) to the (222) reflection.

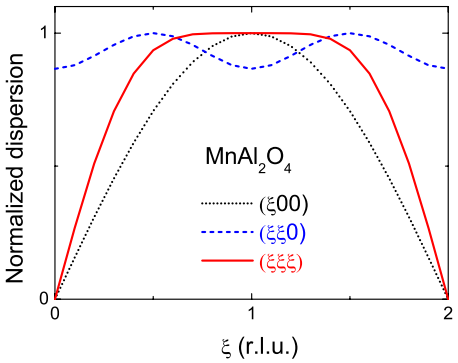

FIG. 2. (Color online) Calculated normalized spin-wave dispersion of $MnAl_2O_4$ for nearest-neighbor exchange along the three principal cubic directions. Details are described in the text.

The overall narrowing in energy of $S(Q,\omega)$ for increasing Q as observed in the corresponding contour plot Fig. 1 is a result of the neutron magnetic form factor and thus confirms the magnetic origin of these scattering contributions. For a more detailed quantitative analysis, cuts of $S(Q,\omega)$ for constant Q values (and constant energy-transfer values, respectively) have been performed within the accessible range of 0.25–5 Å^{-1} in steps of $\Delta Q = 0.25$ Å^{-1}.

The top frame of Fig. 3 shows $S(Q=1.25\ \text{Å}^{-1},\omega)$ of $MnAl_2O_4$ at 160 K. This temperature is not only well above the ordering temperature, but also exceeds the Curie-Weiss temperature θ_{CW}. A purely paramagnetic state with a corresponding quasielastic scattering, whose width is determined by thermal fluctuations, is expected. Neutron-scattering spectra $S(Q=\text{const.},\omega)$ have been fitted using Eqs. (1) and (2), respectively. Good agreement between measured and calculated intensities is found as shown in the upper part of Fig. 3 for $Q = 1.25$ Å^{-1}. Upon approaching the magnetic ordering transition, a change from quasielastic scattering to an inelastic response is expected. Such a change already starts to develop at 50 K, as shown in the midpart of Fig. 3, where the spectra can best be fitted by an additional broad excitation with an energy of approximately 3.5 meV for $Q = 1, 1.25$ and 1.5 Å^{-1} (the other Q values still show a pure quasielastic response). Therefore, 50 K marks the onset temperature for collective magnetic excitations or paramagnons. Below T_N, the magnetic response becomes fully inelastic and is best described by two excitations as shown in the lower frame of Fig. 3. However, this double peak structure is probably related to powder averaging the intrinsic anisotropy of the magnetic excitations. Specific fitting results of $MnAl_2O_4$ for $Q = 1.25$ Å^{-1} are summarized in Fig. 4 showing the tempera-

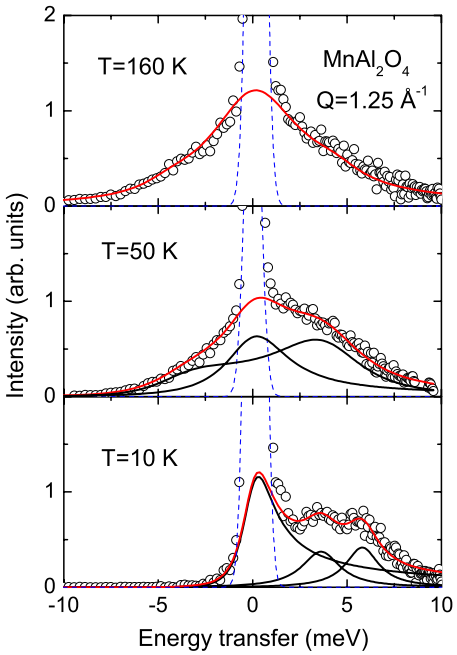

FIG. 3. (Color online) Neutron-scattering spectra at constant wave-vector transfer $Q=1.25$ Å^{-1} of $MnAl_2O_4$ for various temperatures. The blue dashed lines correspond to the elastic line as measured by a vanadium standard, the individual fit components are drawn as black lines and the resulting fit is represented by the full red line.

ture dependence of the quasielastic linewidth Γ, the excitation energies $\omega_j(j=1,2)$ and its corresponding widths $\Gamma_j(j=1,2)$. The quasielastic linewidth documented in Fig. 4 is approximately 4 meV at 150 K and continuously decreases at declining temperatures and levels off at 1 meV, smoothly evolving into the width of the excitations in the ordered state. At the lowest temperatures the two excitations are located at 3.7 and 5.7 meV, respectively.

The data of Fig. 1 already suggest a certain Q dependence of the scattering at elevated temperatures. This is clearly evidenced when plotting the integrated intensities of the Lorentzian fits of the quasielastic scattering for different Q values as shown in Fig. 5. The full line corresponds to the neutron magnetic form factor of Mn^{2+} ions within the dipole approximation[27] which, obviously, cannot account for the measured Q dependence. The peak of the quasielastic scattering intensity around 1 Å^{-1} indicates the presence of AFM correlations even at 160 K. Upon cooling, the Q dependence becomes more pronounced with a clear maximum around 1.25 Å^{-1}. This Q value corresponds to the position of the first magnetic Bragg reflection and below $T_N=40$ K, a spin-wave dispersion emanates from this first Brillouin-zone center, as shown in the two lower frames of Fig. 1.

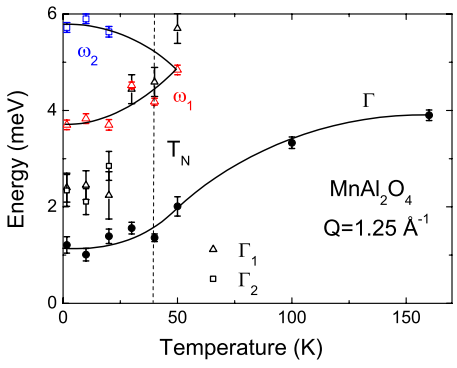

FIG. 4. (Color online) Linewidths and eigenfrequencies of $MnAl_2O_4$ at $Q=1.25$ Å^{-1} versus temperature. Full circles represent the quasielastic linewidth Γ and open symbols show the excitation energy ω_j and linewidth Γ_j of the inelastic damped harmonic oscillator at low temperatures. The Néel temperature is indicated by the vertical dashed line. Full lines are drawn to guide the eyes.

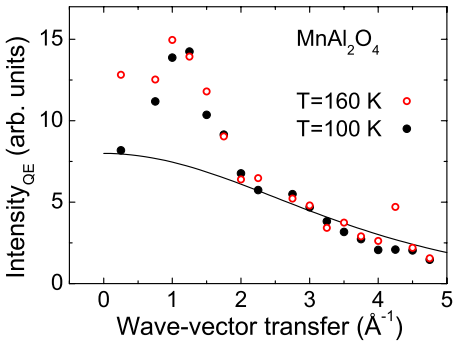

FIG. 5. (Color online) Q dependence of the integrated quasielastic scattering intensities of $MnAl_2O_4$ at 160 K (open red circles) and 100 K (black circles) in the paramagnetic state as resulting from the fits. The solid line corresponds to single-ion behavior according to the neutron magnetic form factor within the dipole approximation.

B. $CoAl_2O_4$

Bulk measurements revealed spin-glass-like anomalies at $T^*=4.8$ K (Ref. 23) and a liquid structure factor of the magnetic scattering in neutron powder-diffraction experiments.[24] An overview of the dynamic structure factor of $CoAl_2O_4$ is shown in Fig. 6. Compared to the Mn-based homolog compound, the magnetic intensities of $CoAl_2O_4$ are located at somewhat lower energy transfers extending up to approximately 8 meV or 90 K (around $Q\approx 1$ Å^{-1}). Taking the experimentally determined Curie-Weiss temperature of 104 K leads then to a mean-field exchange of $J_{MF}=20.8$ K and a scaled exchange constant of $J_1=J_{MF}S(S+1)=78$ K. Thus $T^*/J_1=0.062$ in turn corresponds to $J_2/J_1=0.17$. This value is slightly above the critical ratio of 1/8 and just beyond the range of long-range magnetic order. No evidence of magnetic Bragg peaks was found at $T=1.6$ K. However, the intensity distribution reveals similarities with an ordered compound at 1.6 K [compare $S(Q,\omega)$ with results in $MnAl_2O_4$ at the same temperature].

As reported above, an overall narrowing of $S(Q,\omega)$ is observed in the contour map (Fig. 6) for increasing Q due to the magnetic origin of these scattering contributions. Cuts of $S(Q,\omega)$ for constant Q values (and constant energy-transfer values, respectively) have been performed within the same wave vector range and with identical step width as in the case of $MnAl_2O_4$. A pure quasielastic scattering described by a single Lorentzian line for temperatures $T\geq 100$ K [using

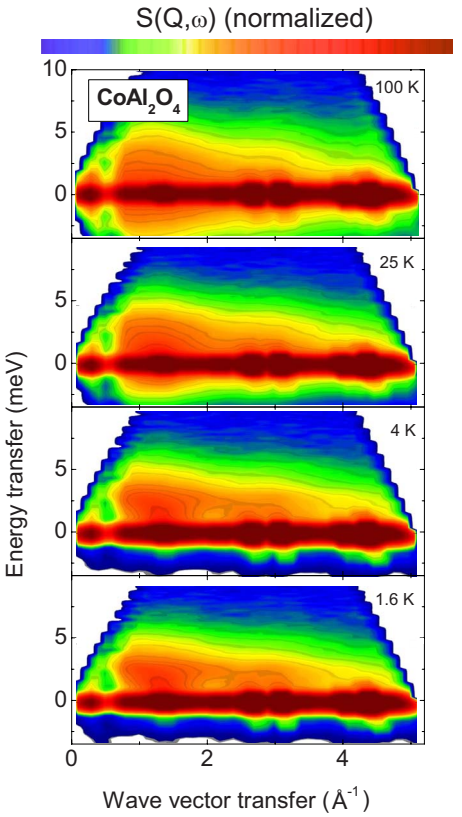

FIG. 6. (Color online) Contour plot of the dynamic structure factor $S(Q,\omega)$ of $CoAl_2O_4$ for various temperatures. Magnetic intensities are shown by a suitable color coding on a logarithmic scale.

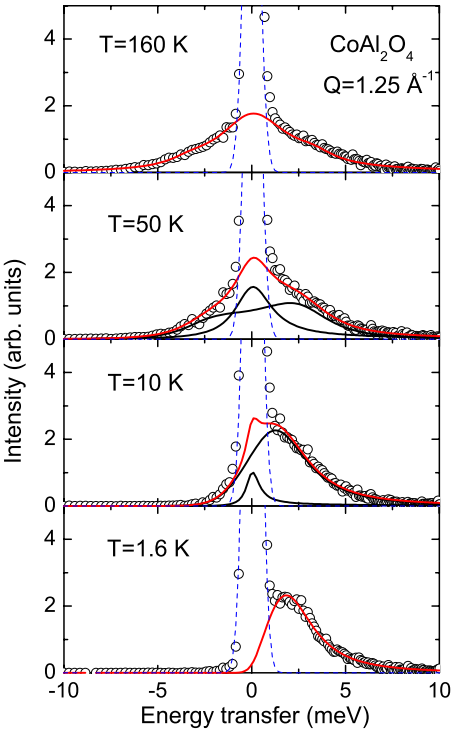

FIG. 7. (Color online) Neutron-scattering spectra of $CoAl_2O_4$ at constant wave-vector transfer $Q=1.25$ Å^{-1} for various temperatures. The blue dashed lines correspond to the elastic scattering as measured by a vanadium standard, the individual fit components are drawn as black lines and the resulting fit is represented by the full red line.

Eqs. (1) and (2)] can account for the measured intensities, as illustrated in the top frame of Fig. 7. Below $T=50$ K, an additional inelastic component is present. At low temperatures ($T=1.6$, 4, and 10 K) the quasielastic scattering contribution has vanished and the magnetic response becomes purely inelastic with an excitation energy of about 2.5 meV as shown in the lower parts of Fig. 7. The corresponding fitting results are summarized in Fig. 8. The quasielastic linewidth, as in $MnAl_2O_4$, decreases upon declining temperatures (roughly following a linear Korringa behavior) and spectral weight is smoothly transferred to the inelastic line of the magnetic excitations at low temperatures. The excitation energies are below those of the manganese spinel.

In contrast to $MnAl_2O_4$, the Q dependence of the integrated intensities of the quasielastic scattering roughly follow the neutron magnetic form factor of a Co^{2+} ion (not shown). Albeit a significant broadening, the magnetic scattering intensities clearly emanate from the elastic line and form bows resembling a magnonlike dispersion along with a change from a quasielastic to an inelastic magnetic response at low temperatures. Despite the absence of long-range magnetic order, the dynamic structure factor of $CoAl_2O_4$ reveals features of collective magnetic excitations. This is in contrary to a complete spin-glass freezing at $T^*=4.8$ K. However, a significant increase in the intensity of the elastic line shows a slowing down of spin fluctuations. The heat capacity exhibits a T^2 temperature dependence between base temperature and 4 K in contrast to canonical spin glasses where a linear temperature dependence is expected. $CoAl_2O_4$ is a cooperative paramagnet located at the border of long-range magnetic order. Entropically stabilized magnetic correlations should mainly point along the 111-direction.[16] In fact, (111) corresponds to a Q-value of 1.34 Å^{-1} in agreement with the experimentally observed maximal magnetic intensity (see Fig. 6). The associated specific heat of entropically stabilized

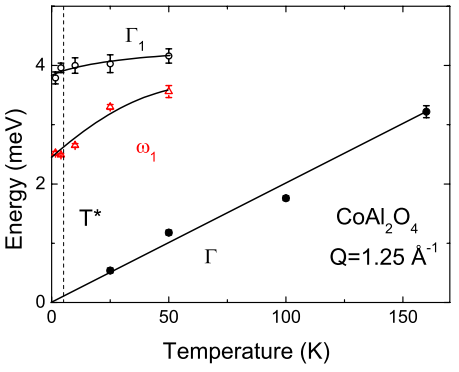

FIG. 8. (Color online) Linewidth and eigenfrequencies of $CoAl_2O_4$ at $Q=1.25$ Å^{-1} versus temperature. Full circles represent the quasielastic linewidth and open symbols show the excitation energy (triangle) and linewidth (circles) of the inelastic damped harmonic oscillator at low temperatures. The characteristic temperature T^* is indicated. The full lines are drawn to guide the eyes.

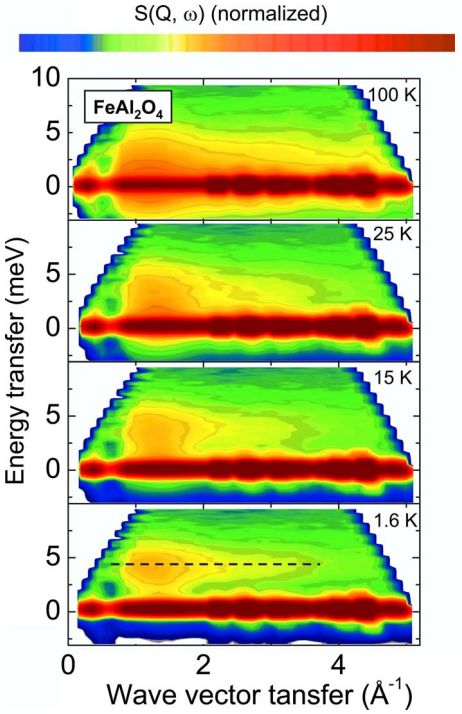

FIG. 9. (Color online) Contour plot of the dynamic structure factor $S(Q,\omega)$ of $FeAl_2O_4$ for various temperatures. Magnetic intensities are shown by a suitable color coding on a logarithmic scale. A band of magnetic excitations with a mean energy of 4 meV without dispersion is indicated by the dashed line.

spin correlations should follow a $T^{7/3}$ dependence in a quantum-mechanical treatment[16] and in reasonable agreement with a T^2 behavior observed experimentally.

C. $FeAl_2O_4$

The corresponding dynamic structure factor of $FeAl_2O_4$ is shown in Fig. 9. The overall energy scale of the magnetic scattering amounts again approximately 10 meV in reasonable agreement with the Curie-Weiss temperature of 130 K determined by magnetic-susceptibility measurements. Within mean-field approximation, $\theta_{CW}=130$ K corresponds to the exchange constant $J_{MF}=16.25$ K for $S=2$ in reasonable agreement with the observed characteristic temperature of $T^*=12$ K, where anomalies in bulk properties indicate a spin-glass-like transition. At 100 K (top frame of Fig. 9) a typical thermally activated quasielastic scattering dominates the magnetic excitation spectrum. Apart from the overall narrowing of $S(Q,\omega)$ on increasing Q due to the magnetic origin of the scattering, some additional slight Q dependence in form of a centering around 1.25 Å^{-1} may be recognized. As described above, cuts of $S(Q,\omega)$ at constant wave vector transfers (constant energy transfers) have been performed for a more detailed analysis. The corresponding neutron-scattering spectra for $Q=1.25$ Å^{-1} are shown in Fig. 10 at various temperatures and the results of the fits are summarized in Fig. 11.

A pure quasielastic scattering in form of a single Lorentzian line [Eqs. (1) and (2) above] is observed for $T\geq 50$ K.

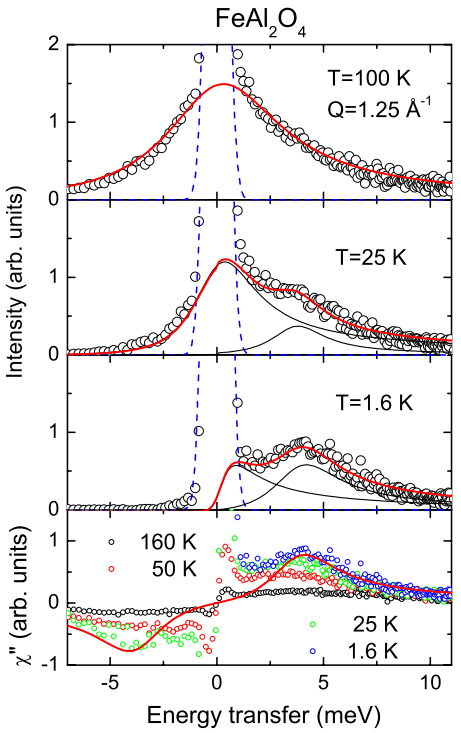

FIG. 10. (Color online) Structure factor $S(\omega)$ at constant wave vector transfer $Q=1.25$ Å^{-1} of $FeAl_2O_4$ for various temperatures. The blue dashed lines correspond to the elastic line as measured by a vanadium standard, the individual fit components are drawn as black lines and the resulting fit is represented by the full red line. The lowest frame shows a simultaneous plot of $\chi''(\omega)$ for four different temperatures to evidence the evolution of a spin gap.

Upon cooling, the magnetic response becomes inelastic, as illustrated for $T=25$ K in Fig. 10. This behavior is reflected by the onset of a significant Q dependence in $S(Q,\omega)$ (Fig. 9). On further cooling to 15 K, the dynamic structure factor of $FeAl_2O_4$ exhibits a more pronounced Q dependence resembling the evolution of a spin-wave dispersion, as observed in the Co homolog compound. However, upon cooling to 4 and 1.6 K respectively, a remarkably distinct

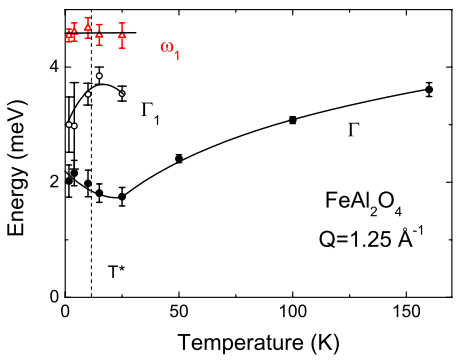

FIG. 11. (Color online) Linewidth and eigenfrequencies of $FeAl_2O_4$ at $Q=1.25$ Å^{-1} versus temperature. Full circles represent the quasielastic linewidth and open symbols show the excitation energy (triangles) and linewidth (circles) of the inelastic damped harmonic oscillator at low temperatures. The characteristic temperature T^* is indicated. Full lines are drawn to guide the eyes.

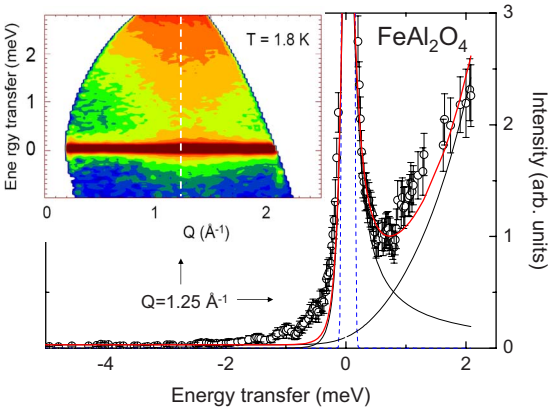

FIG. 12. (Color online) High-resolution spectrum of $FeAl_2O_4$ at $T=1.8$ K revealing an energy pseudogap for magnetic excitations. The dynamic structure factor (full red line) is the sum of a quasielastic and an inelastic contribution (thin black lines). It is the result of a cut in the low-energy or low-Q region of $S(Q,\omega)$ as shown in the inset at constant $Q=1.25$ Å^{-1} (vertical dashed white line).

behavior is realized. The magnetic response becomes completely inelastic (see lower part of Fig. 10) but rather localized exhibiting an island structure in $S(Q,\omega)$ (compare with Fig. 9) accompanied by an opening of a spin gap of approximately 4 meV being characteristic of a spin liquid. The temperature-induced evolution of the energy gap in the spin excitation spectrum is nicely evidenced in the bottom frame of Fig. 10 by plotting $\chi''(\omega)$ [corresponding to $S(Q=1.25$ Å$^{-1},\omega)$ without the detailed balance factor] simultaneously for various temperatures. This peculiar behavior of $FeAl_2O_4$ at low temperatures was further investigated by additional high-resolution measurements on the time-of-flight spectrometer IN6 employing cold neutrons with an incident wavelength of 5.1 Å. The inset of Fig. 12 shows the corresponding low-energy transfer or low-Q region of the dynamic structure factor $S(Q,\omega)$ of $FeAl_2O_4$ at 1.8 K. The inelastic-scattering contributions due to magnetic excitations are clearly separated from the elastic line. A cut of $S(Q,\omega)$ at constant $Q=1.25$ Å^{-1} is performed and indicated by the vertical dashed line of the inset. The resulting spectrum is displayed in the main frame of Fig. 12. The magnetic excitations are isolated from the elastic line but the intensity does not vanish completely, thus revealing an energy pseudogap with a minimum around $\Delta \approx 0.7$ meV. Similar to $CoAl_2O_4$, a broad maximum of the specific heat around $T^*=12$ K followed by a T^2-temperature dependence toward lower temperatures together with a splitting of the fc-zfc magnetization and the absence of long-range magnetic order (absence of magnetic Bragg peaks in neutron powder diffraction) has been taken as evidence for a spin-glass-like state in $FeAl_2O_4$.[23] In fact, as in case of $CoAl_2O_4$ we find a strong increase in the intensity of the elastic line. This holds true for the high-resolution measurements performed on IN6 with an energy resolution of 70 μeV, implying a slowing down of magnetic fluctuations below 10^{-10} s. A detailed analysis of the spin-spin-correlation function on the basis of a previous neutron powder-diffraction study, supplemented by susceptibility and Mössbauer measurements[28] also indicated a spin-glass state for $FeAl_2O_4$. However, the physical properties of aluminum-oxide spinels depend sensitively on the degree of cation inversion. All presently investigated samples have been synthesized at moderate temperatures and slow cooling rates to minimize inversion with a residual value of approximately 7%–8%. The rather strong indications of a spin-glass state observed previously[28] were measured on samples with a high degree of inversion of about 17%. It is well known that spin-glass-like properties demand both frustration as well as a sufficient degree of disorder which can be provided by cation inversion.

III. SUMMARY AND CONCLUSIONS

We have presented results of a detailed neutron-scattering investigation of the frustrated spinels MAl_2O_4(M =Mn,Co,Fe). All of these three spinel compounds are located at the border of long-range magnetic order with distinct emergent behavior in their corresponding magnetic excitation spectra. The essential difference is the additional orbital degree of freedom in $FeAl_2O_4$ as compared to the effective spin-only ions Mn^{2+} and Co^{2+} in $MnAl_2O_4$ and $CoAl_2O_4$, respectively. The overall energy-transfer range of the magnetic scattering reflects the strength of the leading magnetic exchange, which corresponds to the Curie-Weiss temperatures determined by magnetic measurements, and in turn scales with the spin value of the respective compound. $MnAl_2O_4$ reveals long-range magnetic order but with a significant additional paramagnetic component. Contrarily, $CoAl_2O_4$ fails to develop long-range magnetic order. It shows strong, but only short-ranged spin correlations and collective magnetic excitations but remains paramagnetic. It is therefore a typical example of a cooperative paramagnet among the class of frustrated magnets. A significant increase in the elastic intensity at low temperatures is indicative for a slowing down of magnetic fluctuations and the proximity to a spin-glass ground state. Within the theoretical model calculations of a frustrated antiferromagnet on a diamond lattice, $CoAl_2O_4$ exhibits a coupling strength ratio $J_2/J_1=0.17$ with a spiral spin-liquid state and magnetic correlations entropically stabilized predominantly along the 111 direction.[16] Magnetic entropy seems to also be responsible for the peculiar power-law behavior of the specific heat at low temperatures. Accordingly, $MnAl_2O_4$ exhibits a ratio of about $J_2/J_1 \approx 0.09$ thus just developing an AFM Néel ground state with a reduced ordering temperature and an additional paramagnetic component. The magnetic excitation spectra of $MnAl_2O_4$ can be well described by a spin-wave dispersion along the (111) direction, dominated by nearest-neighbor interactions. The orbital degree of freedom in $FeAl_2O_4$ makes model calculations difficult. Bulk measurements reveal the presence of orbital contributions.[23] The inelastic neutron-scattering measurements $FeAl_2O_4$ show strong, but short-ranged AFM correlations and the evolution of an energy pseudogap in its spin excitation spectrum.

The strongly gapped excitation spectrum of $FeAl_2O_4$, as documented in Fig. 9 by $S(Q,\omega)$ at 1.6 K, probably results from the orbital degrees of freedom. Fe^{2+} in a tetrahedral environment is Jahn-Teller-active via an electron hole in the lower doublet. There is no experimental evidence for the

occurrence of a cooperative Jahn-Teller transition, indicating that the orbital degeneracy exists down to the lowest temperatures. However we expect a strong influence of spin-orbit coupling (SOC) to the crystal-field derived ground state. From optical-absorption experiments on Fe^{2+} defects at the *A* site of nonmagnetic spinel compounds,[29] it is known that the crystal-field splitting $\Delta=2500\ \mathrm{cm}^{-1}$ ($1\ \mathrm{cm}^{-1}$ corresponds to 0.124 meV). Additionally, the SOC splits the ground doublet into five levels which are separated by $\delta=6\lambda^2/\Delta$,[30] with λ being the spin-orbit coupling constant. The influence of magnetic exchange or of an effective spin-spin coupling has been neglected here. If we assume that the almost nondispersive excitation located roughly at $\hbar\omega=3.8$ meV at 1.6 K in Fig. 9 results from the lowest level of the spin-orbit split ground state, and taking the crystal-field separation as indicated above, we calculate a spin-orbit coupling constant of approximately $110\ \mathrm{cm}^{-1}$, which seems to be a reasonable result for Fe^{2+} in a tetrahedral environment. A spin-orbit coupling constant of $70\ \mathrm{cm}^{-1}$ has been determined for Fe^{2+} substituted at the *A* site of diamagnetic $CdIn_2S_4$.[29] Of course in the case of $FeAl_2O_4$, the excitation spectra are further complicated by the presence of magnetic exchange, but the size of the thus determined spin-orbit coupling may serve as a first evaluation. A gapped excitation spectrum has also been observed in $FeSc_2S_4$. However in this case the magnetic excitation spectrum is strongly dispersive and magnetic exchange plays a considerable role.

This situation has been described as spin-orbital liquid close to a quantum critical point,[31] by taking purely electronic Kugel-Khomskii-type spin-orbital interactions into account, which drive the system toward orbital and magnetic order. A theoretical study of the spin-orbital liquid state in $FeSc_2S_4$ reveals a competition between spin-orbit interactions which favor a nonmagnetic, disordered spin-orbital singlet state and exchange interactions that tend toward an AFM and orbitally ordered state.[31] The two phases are separated by a quantum critical point. The disordered spin-orbital singlet state displays an excitation gap of the order of the Curie-Weiss temperature.[31] Both $FeSc_2S_4$ and the presently investigated $FeAl_2O_4$ reveal spin gaps that are significantly smaller than θ_{CW}. No direct experimental evidence of orbital fluctuations can be extracted from the present neutron-scattering data. At present, it is unclear why $FeAl_2O_4$ with a Curie Weiss temperature of 120 K reveals no or only weak indications of magnetic dispersion, while $FeSc_2S_4$, with a Curie-Weiss temperature of 50 K, reveals strongly dispersive magnon excitations at low temperatures. This fact could be explained when assuming a much weaker spin-orbit coupling in the later compound. An orbital excitation has been detected in $FeSc_2S_4$ close to 2 meV.[20] Assuming the same size of the crystal-field splitting ($\Delta=2500\ \mathrm{cm}^{-1}$) results in a spin-orbit coupling of the order of $80\ \mathrm{cm}^{-1}$. To explain the significantly different results in $FeSc_2S_4$ and $FeAl_2O_4$ probably the coupling to the lattice through phonon modes has to be taken into account. The orbital-like excitation in $FeSc_2S_4$ has been explained on the basis of vibronic models.[20]

As in the case of the Co-based compound, a strong increase in the elastic intensity is observed in $FeAl_2O_4$ at low temperatures, due to a slowing down of magnetic fluctuations consistent with a proximate spin-glass state. This behavior is most likely related to a moderate degree of inversion, as in samples with a high fraction of inversion a completely frozen spin-glass state is realized. The additional high-resolution measurements for $FeAl_2O_4$ set an upper limit of 10^{-10} s for the time scale of spin fluctuations. However, recent μSR experiments on $M\mathrm{Al}_2\mathrm{O}_4(M=\mathrm{Mn},\mathrm{Co},\mathrm{Fe})$ clearly show that the Fe compound exhibits a faster relaxation than the Co compound.[32] Further inelastic neutron-scattering experiments on single crystals are needed to fully understand the magnetic excitations in the *A*-site spinels $M\mathrm{Al}_2\mathrm{O}_4(M=\mathrm{Mn},\mathrm{Co},\mathrm{Fe})$.

ACKNOWLEDGMENTS

This work was supported by the Deutsche Forschungsgemeinschaft DFG via Project No. SFB 484, Augsburg and research unit 960 "Quantum phase transitions."

*alexander.krimmel@physik.uni-augsburg.de

[1] A. P. Ramirez, in *Handbook of Magnetic Materials*, edited by K. H. J. Buschow (Elsevier Science, Amsterdam, 2001), Vol. 13, p. 423.
[2] B. Canals and C. Lacroix, Phys. Rev. Lett. **80**, 2933 (1998).
[3] A. P. Ramirez, A. Hayashi, R. J. Cava, R. Siddhartan, and B. S. Shastry, Nature (London) **399**, 333 (1999).
[4] S. P. Bramwell and M. J. P. Gringas, Science **294**, 1495 (2001).
[5] A. J. Garcia-Adeva and D. L. Huber, Phys. Rev. Lett. **85**, 4598 (2000).
[6] P. G. Radaelli, Y. Horibe, M. J. Gutmann, H. Ishibashi, C. H. Chen, R. M. Ibberson, Y. Koyama, Y.-S. Hor, V. Kiryukhin, and S.-W. Cheong, Nature (London) **416**, 155 (2002).
[7] S.-H. Lee, C. Broholm, W. Ratcliff, G. Gasparovic, Q. Huang, T. H. Kim, and S.-W. Cheong, Nature (London) **418**, 856 (2002).
[8] S. Kondo, D. C. Johnston, C. A. Swenson, F. Borsa, A. V. Mahajan, L. L. Miller, T. Gu, A. I. Goldman, M. B. Maple, D. A. Gajewski, E. J. Freeman, N. R. Dilley, R. P. Dickey, J. Merrin, K. Kojima, G. M. Luke, Y. J. Uemura, O. Chmaissem, and J. D. Jorgensen, Phys. Rev. Lett. **78**, 3729 (1997).
[9] A. Krimmel, A. Loidl, M. Klemm, S. Horn, and H. Schober, Phys. Rev. Lett. **82**, 2919 (1999).
[10] E. Berg, E. Altman, and A. Auerbach, Phys. Rev. Lett. **90**, 147204 (2003).
[11] T. Rudolf, Ch. Kant, F. Mayr, J. Hemberger, V. Tsurkan, and A. Loidl, New J. Phys. **9**, 76 (2007).
[12] M. Reehuis, A. Krimmel, N. Büttgen, A. Loidl, and A. Prokofiev, Eur. Phys. J. B **35**, 311 (2003).
[13] O. Tchernyshyov, R. Moessner, and S. L. Sondhi, Phys. Rev. Lett. **88**, 067203 (2002).
[14] Y. Yamashita and K. Ueda, Phys. Rev. Lett. **85**, 4960 (2000).
[15] P. W. Anderson, Phys. Rev. **102**, 1008 (1956).
[16] D. Bergman, J. Alicea, E. Gull, S. Trebst, and L. Balents, Nat. Phys. **3**, 487 (2007).

[17] A. Krimmel, M. Mücksch, V. Tsurkan, M. M. Koza, H. Mutka, C. Ritter, D. V. Sheptyakov, S. Horn, and A. Loidl, Phys. Rev. B **73**, 014413 (2006).
[18] V. Fritsch, J. Hemberger, N. Büttgen, E.-W. Scheidt, H.-A. Krug von Nidda, A. Loidl, and V. Tsurkan, Phys. Rev. Lett. **92**, 116401 (2004).
[19] N. Büttgen, J. Hemberger, V. Fritsch, A. Krimmel, M. Mücksch, H.-A. Krug von Nidda, P. Lunkenheimer, R. Fichtl, V. Tsurkan, and A. Loidl, New J. Phys. **6**, 191 (2004).
[20] A. Krimmel, M. Mücksch, V. Tsurkan, M. M. Koza, H. Mutka, and A. Loidl, Phys. Rev. Lett. **94**, 237402 (2005).
[21] R. Fichtl, V. Tsurkan, P. Lunkenheimer, J. Hemberger, V. Fritsch, H. A. Krug von Nidda, E. W. Scheidt, and A. Loidl, Phys. Rev. Lett. **94**, 027601 (2005).
[22] N. Büttgen, A. Zymara, C. Kegler, V. Tsurkan, and A. Loidl, Phys. Rev. B **73**, 132409 (2006).
[23] N. Tristan, J. Hemberger, A. Krimmel, H. A. Krug von Nidda, V. Tsurkan, and A. Loidl, Phys. Rev. B **72**, 174404 (2005).
[24] A. Krimmel, V. Tsurkan, D. Sheptyakov, and A. Loidl, Physica B **378-380**, 583 (2006).
[25] http://www.ill.fr/data_-treatment/lamp/front.html.
[26] B. Fåk and B. Dorner, Physica B **234-236**, 1107 (1997).
[27] J. Brown, *International Tables for Crystallography* (Kluwer Academic, Dordrecht, 2006), Vol. C, p. 454.
[28] J. L. Soubeyroux, D. Fiorani, E. Agostinelli, S. C. Bhargava, and J. L. Dormann, J. Phys. (France) **49**(C8), 1117 (1988).
[29] S. Wittekoek, R. P. van Stapele, and A. W. J. Wijma, Phys. Rev. B **7**, 1667 (1973).
[30] J. T. Vallin, Phys. Rev. B **2**, 2390 (1970).
[31] G. Chen, L. Balents, and A. P. Schnyder, Phys. Rev. Lett. **102**, 096406 (2009).
[32] G. M. Kalvius (private communication).